

# Embodied Crowd Counting

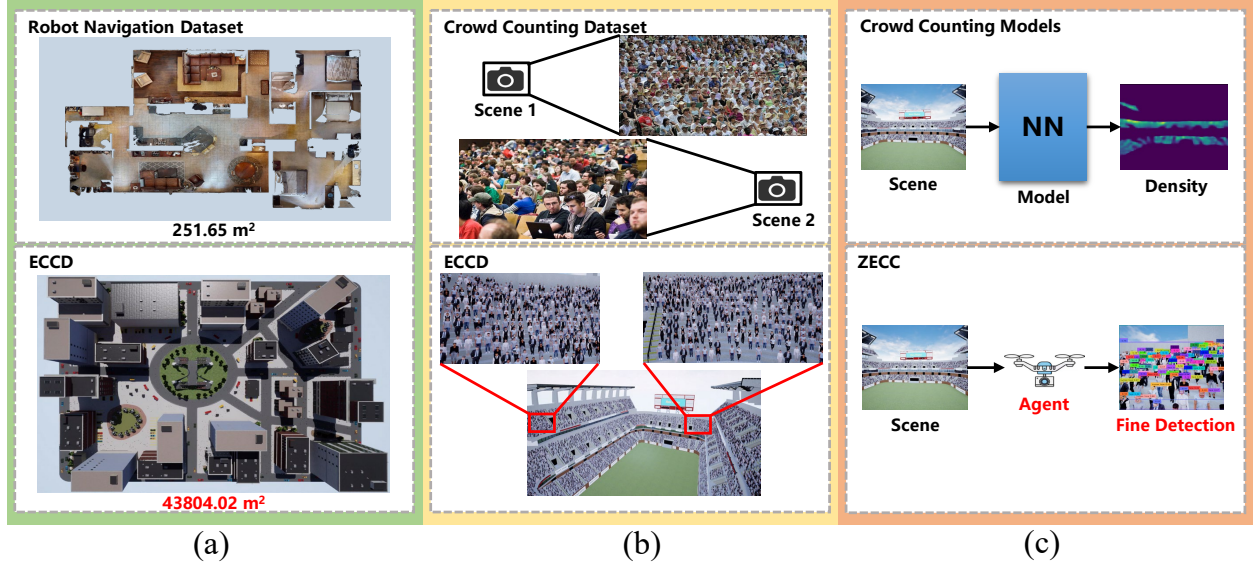
Runling Long<sup>1</sup>Yunlong Wang<sup>1</sup>  
Weili Guan<sup>1</sup>Jia Wan<sup>1\*</sup>  
Antoni B. Chan<sup>2</sup>Xiang Deng<sup>1</sup>  
Liqiang Nie<sup>1</sup>Xinting Zhu<sup>2</sup>

Figure 1: Comparisons between our dataset&model and others. (a) Comparison of environment areas between existing robot navigation datasets and ours. Our dataset features large-scale outdoor crowd scenes. (b) Comparison of lenses interactivity between existing crowd counting datasets and ours. Our dataset includes a 3D structural environment for each scenario, enabling interaction with agents. (c) Comparison of methods between traditional crowd counting models and ours. We propose using agent navigation to achieve precise detection in previously unexplored faraway areas.

## Abstract

Occlusion is one of the fundamental challenges in crowd counting. In the community, various data-driven approaches have been developed to address this issue, yet their effectiveness is limited. This is mainly because most existing crowd counting datasets on which the methods are trained are based on passive cameras, restricting their ability to fully sense the environment. Recently, embodied navigation methods have shown significant potential in precise object detection in interactive scenes. These methods incorporate active camera settings, holding promise in addressing the fundamental issues in crowd counting. However, most existing methods are designed for indoor navigation, showing unknown per-

formance in analyzing complex object distribution in large scale scenes, such as crowds. Besides, most existing embodied navigation datasets are indoor scenes with limited scale and object quantity, preventing them from being introduced into dense crowd analysis. Based on this, a novel task, Embodied Crowd Counting (ECC), is proposed. We first build up an interactive simulator, Embodied Crowd Counting Dataset (ECCD), which enables large scale scenes and large object quantity. A prior probability distribution that approximates realistic crowd distribution is introduced to generate crowds. Then, a zero-shot navigation method (ZECC) is proposed. This method contains a MLLM driven coarse-to-fine navigation mechanism, enabling active Z-axis exploration, and a normal-line-based crowd distribution analysis method for fine counting. Experimental results against baselines show that the proposed method achieves the best trade-off

<sup>1</sup> Harbin Institute of Technology (Shenzhen)

<sup>2</sup> City University of Hong Kong

\*Corresponding Author

*between counting accuracy and navigation cost.*

## 1. Introduction

Crowd counting is critical for public safety and urban planning [21]. One main challenge in this field is occlusion. It can be categorized into two aspects: overlap and invisibility. Overlap refers to the high density of people stacked together, making it difficult to distinguish each individual from some viewpoints, while invisibility indicates that the current camera position is obstructed, such as being blocked by buildings, or far from the crowds so that the target cannot be detected clearly. To summarize, these situations are caused by a poor observation point. Existing methods try to solve these challenges from several perspectives, such as using multi-scale feature extraction [20], body part detection [26] or multi-camera fusion [49, 50]. Datasets are also expanded for enhancing method performance [19, 36, 43, 51]. In general, these methods or datasets either try to enhance learned model representation, or expand the camera sensing range by introducing multi-view settings. Yet, their passive camera settings do not fully solve the occlusion challenge in crowd counting, especially in cases where crowds exceed the sensing range, or no cameras are set to detect completely obscured crowds. These issues restrict passive-camera-based methods in practice.

Recent development in Embodied AI brings perspectives to solve the occlusion challenge in crowd counting. It has been demonstrated to possess significant potential in enhancing scene exploration and object detection. Aspects such as Vision-Language-Navigation (VLN) have been directed towards equipping mobile robots with human-like perception abilities, resulting in remarkable performance in exploring scenes and detecting objects in open environments [4, 7, 9, 52]. The active camera settings in VLN is promising to solve the fundamental challenges in crowd counting, since it can optimize observation point to mitigate overlap and invisibility caused by poor camera position setting. Yet most VLN benchmarks [1, 3, 40, 44] are indoor environments with limited exploration space (e.g., no Z-axis action options) and relatively small object quantity. And the performance of such methods remains unknown for detecting crowds with a large quantity and complex distribution in large-scale scenes. This results in a significant gap between VLN and crowd counting, as in practice, crowds often appear in large spaces with varying distribution.

To address the issues mentioned above, we first define a novel task, Embodied Crowd Counting (ECC). This task integrates crowd counting into the Zero-shot

Object-Goal Navigation task (ZSON) in VLN [28]. It is designed for large-scale scenes with a large object quantity. A testing environment, Embodied Crowd Counting Dataset (ECCD), is then developed for this task. Compared to existing crowd counting and VLN datasets, this test environment has the following features: 1) It supports 60 distinct and diverse large-scale outdoor scenes. Each scene covers an area up to  $40,000 m^2$ , with target quantity up to 15,000. 2) It uses a prior distribution, Poisson Point Process [11], for crowd quantity distribution modeling, which approximates realistic crowd situations.

Based on this platform, we develop a method, Zero-shot Embodied Crowd Counting (ZECC), to conduct crowd counting in ECCD. Compared to existing crowd counting methods and VLN methods, ZECC has the following features: 1) It uses active camera setting to solve fundamental challenges in crowd counting, transferring the detection task to an exploration task; 2) It consists of a coarse-to-fine navigation mechanism which uses common sense of Multi-Modal-Large-Language-Model (MLLM) to analyze the surrounding environment and plan Z-axis exploration, leveraging advantages of 6 degrees of freedom (6-DoF) to avoid low-altitude obstacles and gain border sight, thus achieving efficient exploration; 3) It consists of a crowd distribution analysis mechanism which transfers the complex crowd distribution to simple surfaces. The normal lines of the surfaces are used to generate fine observation points, which are used to mitigate the influence of overlap and invisibility, enabling accurate crowd counting.

The contributions of this work can be summarized as follows:

- We present an innovative task called ECC, specifically designed to address the challenges of occlusion and multi-scale complexities that are prevalent in conventional crowd counting methods.
- A new dataset called ECCD has been collected to redefine the landscape of crowd analysis. Unlike traditional crowd counting and VLN datasets, it features large-scale outdoor crowd scenes with interactive capabilities.
- ZECC is proposed to use MLLM for Z-axis exploration, reducing costs while ensuring detection performance. By utilizing normal lines to calculate navigation points, this approach eliminates overlap and enhances visibility in crowds.
- Experiments show that the proposed method outperforms the baseline methods in various testing environments.

## 2. Related Work

### 2.1. Crowd Counting

Crowd-counting algorithms have greatly benefited from large-scale, high-quality datasets like UCF-CC50 [18] and UCF-QNRF [19]. These foundational datasets have facilitated the creation of subsequent collections focused on dense crowd imagery, such as ShanghaiTech [51], JHU-CROWD++ [36], NWPU-Crowd [43]. However, the images in these datasets are generated from fixed cameras. In contrast, ECCD provides interactive capabilities while maintains diverse crowd distribution.

Methods like [5, 20, 24, 24, 51] leverage crowd distribution prior in an image, or using attention maps to learn dependency. Recent multi-modal approaches [10, 29, 42, 47] leverage vision-language models to transfer image-text knowledge to dense crowd prediction. While these models improve long range and overlapping small target detection ability, their performance are restricted in practical if overlap reaches extreme level. Recent efforts expand spatial coverage. These works include multi-view systems [17, 32] that use multi camera to capture images from larger scale scenes. Others like [14, 15] use recorded video to conduct crowd analysis. While these are important advances on solving the fundamental challenges in crowd counting against the single-fix-image-based methods, their camera setting is still predefined by the dataset and cannot be adjusted when inferring. This cannot ensure fully exploration in a large environment. ZECC allows active exploration, which is fundamentally different from existing methods.

### 2.2. Embodied Navigation

Many traditional robot navigation methods were developed using conventional navigation datasets like KITTI [12] and SUN RGB-D [38]. Beyond these foundational datasets, [33, 44] provide 3D indoor environments for navigation and interaction tasks. These datasets are limited with their small scale size and small object quantity. Recent datasets have been created towards outdoor navigation like AerialVLN [25], and CityNav [23]. However, they are designed for VLN tasks without consideration of object quantity. Compared to these datasets, ECCD simultaneously supports large scale outdoor scenes and large object quantity with diverse distribution.

Efficient exploration using mobile robots remains a crucial challenge in vision and robotics. [13, 16, 30, 38] have developed human-like cognitive maps, enabling autonomous path learning in unknown environments. Other approaches like [2, 6, 31] use reinforcement learning to develop exploration policies. Recently, [48] applied

video-based visual-language models to plan sequential actions in VLN. And [27, 53] presented zero-shot models that utilizes natural language instructions to guide agents through environments without prior environment-specific training. However, the methods mentioned above are for indoors navigation without Z-axis moving ability. This restricts their ability in large scale outdoor scenes. Recently, methods like [25, 45] introduce 6-DoF in outdoor VLN. Yet they are designed for instruction following task, in which the movement is restricted by human language. Besides, they lack ability to analyze crowds with large quantity and complex distribution. In contrast, ZECC is the first self-motivated agent in 6-DoF and can handle crowds simultaneously.

## 3. Method

### 3.1. Problem Definition

To ensure the interactive with environment for accurately crowd counting in vast outdoor environments, we propose an innovative task called Embodied Crowd Counting (ECC). In ECC, an agent is first deployed in an unknown environment. At time step  $t$ , the input of the agent is RGB-D observations  $O_t$  along with its pose  $p_t$ . Based on this information, the agent predicts navigation point  $p \in \mathbb{R}^3$  to a drone at time step  $t$  and the drone moves to  $p$ . During exploration, the agent is allowed to record observations that help with crowd counting. When the agent decides to stop, it outputs an integer that represents its crowd counting result. The counting error and travel distance are calculated to assess the agent's performance. ECC can be considered analogous to the ZSON task, since they both require an agent to detect targets in an unexplored environment without additional assistance. However, there are several differences. The task setting differences are: 1) The object category  $G$  in ZSON is limited to crowd in ECC. 2) The step limitation in ZSON is removed in ECC. 3) The evaluation criterion in ECC is changed to counting error and travel distance. These differences do not prevent the availability of most recent ZSON methods in ECC by conducting minor modifications. However, agents should face essential differences in ECC: 1) Z-axis is available, which is not considered by most recent ZSON methods. 2) Complex crowd distributions exist, including heavy occlusions, while ZSON methods only consider objects with small quantity. Current ZSON methods show unknown performance under such differences, and new methods should be considered in ECC. Note that ECC is different from the instruction following tasks in VLN such as [25, 45], since these tasks require natural language assistance to drive the agent.

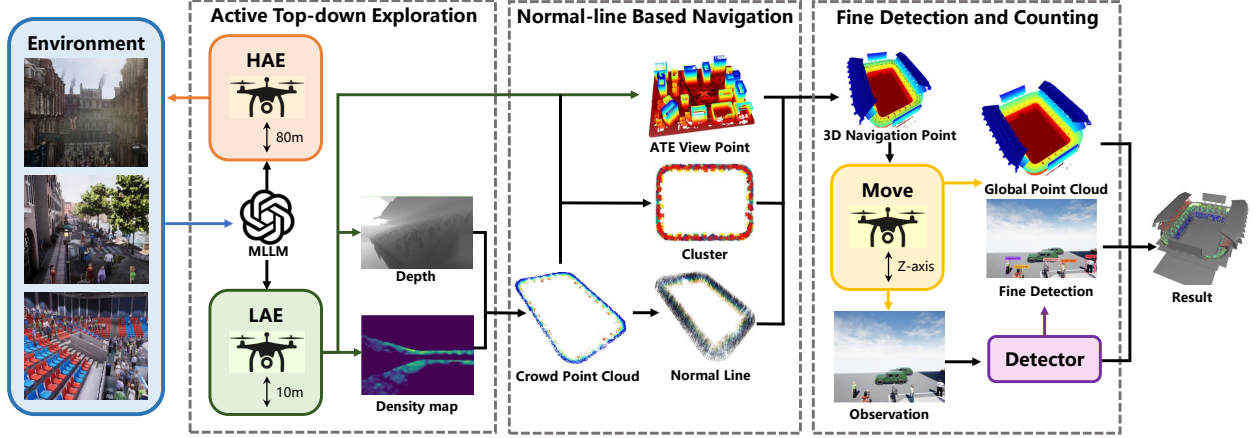


Figure 2: The proposed framework for ZECC consists of several key steps. First, we utilize an exploration strategy based on FBE to create a global crowd distribution by generating a target point cloud. Next, we apply a Gaussian Mixture Model (GMM) clustering to identify the representative centers of the global target point cloud and determine the final navigation points based on potential navigation directions. Finally, we integrate detection results obtained from various detectors with depth observations, mapping these to the global point cloud. The number of filtered targets is then counted and recorded as the final result for the crowd.

### 3.2. Embodied Crowd Counting Dataset (ECCD)

We propose a new dataset called ECCD to support algorithm design and evaluation for the community. ECCD is developed using Unreal Engine 4. This platform enables programmable environment construction, allowing scene richness and scalability. The characteristics of ECCD are as follows:

**Diversity.** Since different environments have different layouts, crowd distributions, and quantities reflect different challenges, ECCD is designed to contain diverse scenes. This dataset contains 60 distinct environments. Also, ECCD has an area up to  $40,000 m^2$ , reaches a height up to  $50 m$ , and allows for the simultaneous presence of over 15,000 targets within a single scene. This is significantly different from existing robot navigation datasets, such as [33] which offers environments with an average navigable space of  $1,000 m^2$ , and crowd counting datasets, such as [51] which contains 1,198 annotated images captured with static cameras and a total of 330,165 individuals.

**Realism.** The ECCD is designed to simulate large-scale outdoor crowd scenarios in reality, in order to ensure practical effectiveness of systems built on ECCD, as shown in Figure 3. Environments like a city, a stadium, and a parking lot are simulated. Additionally, the environments support a complex structure of buildings in real life, such as multiple floors and bleachers. These features allow ECCD to reflect challenges in reality.

**Crowd generation mechanism.** To model real chal-



Figure 3: ECCD is designed to realistically mimic building and crowd distribution. On the left are samples from ECCD, and on the right are the real scenes.

lenges in crowd counting, ECCD uses Poisson Point Process for crowd quantity distribution modeling [11]. In ECCD, Blocks are placed in the simulator to present potential areas where crowds may exist. Then, for each block  $\mathcal{U} \subset \mathbb{R}^2$ , the process is defined as:

$$\mathbb{P}(N(\mathcal{U}) = k) = \frac{(\lambda \cdot |\mathcal{U}|)^k}{k!} e^{-\lambda \cdot |\mathcal{U}|}, \quad k \in \mathbb{N}, \quad (1)$$

where  $N(\mathcal{U})$  denotes the number of individuals in block  $\mathcal{U}$ ,  $\lambda$  represents the crowd density set by human experts

according to the environment semantics, and  $|\mathcal{U}|$  is the area of the block. This ensures ECCD generates crowds that approximate real situations. By comparison, existing simulators based on UE4, such as AirVLN and OpenUAV, do not consider object quantity and distribution.

### 3.3. Zero-shot Embodied Crowd Counting (ZECC)

#### 3.3.1 Overview

Previous embodied navigation agents are designed for indoor environments [27], or relying on language assistance [25, 45], making them restricted in large-scale outdoor scenes. Under such context, a zero-shot agent, ZECC, which can actively control altitude and conduct crowd analysis, is proposed. As illustrated in Figure 2, the method consists of 2 components, Active Top-down Exploration (ATE) and Normal-line based Navigation (NLBN). ATE is designed for adjusting agent altitude for efficient coarse crowd distribution estimation, and NLBN estimates normal lines on top of crowd for accurate crowd observation, alleviating occlusion.

#### 3.3.2 Active Top-down Exploration (ATE)

Crowds are often concentrated in specific areas, such as roads and squares, making it unnecessary to explore every region of the environment. To address this, ATE is proposed to estimate the global distribution of crowds from a high altitude. This approach aims to improve efficiency by focusing exploration efforts on the most relevant areas and avoiding unnecessary locations. In particular, high-altitude exploration (HAE) brings a broader field of view for decision making, as well as relatively less exploration cost since obstacles are often sparse in high altitude. While low-altitude exploration (LAE) provides close range observation for clear target detection. It is essential for the agent to plan HAE and LAE to achieve efficiency and accuracy simultaneously. Therefore, ATE leverages the Z-axis mobility of outdoor agents and the common sense of multi-modal large language model (MLLM) to switch between HAE and LAE by local environment layout reasoning. Then, the crowd distribution is estimated by crowd counting model to predict density maps in the environment.

Specifically, the agent collects observations  $O_t = \{o_t^1, \dots, o_t^c\}$  and pose  $p_t$  at time step  $t$ , where  $c$  indicates the camera number of the agent. Then, a MLLM is prompted by using the observations and text prompts to conduct environment layout reasoning. The MLLM is asked to predict whether current location is valuable for LAE, by referring current crowd appearance and obstacle

layout. This process is formulate as:

$$s_t = \text{MLLM}(O_t; I), \quad (2)$$

where  $\text{MLLM}(\cdot)$  is the inference process and  $I$  is the prompt.  $s_t \in [0, 1]$ . If  $s_t > 0.5$ , the agent will adjust its altitude for LAE. After switching altitude strategy, the agent will conduct regular exploration. For HAE, one of the frontiers between explored and unknown areas is selected as navigation point. For LAE, the agent will keep exploring frontiers until areas within its field of view during HAE are fully explored. During LAE, once the agent reaches a frontier  $f$ , it gathers observations  $O_f = \{o_f^1, \dots, o_f^c\}$ , and a crowd counting model predicts crowd density maps on the observations. Then the density maps are projected onto the global point cloud to form a global crowd distribution. This is formulated as:

$$d_f = \text{P}(\text{G}(O_f), p_f), \quad (3)$$

where  $\text{P}(\cdot)$  is the projection operation,  $\text{G}(\cdot)$  is a crowd counting model, and  $p_f$  is the agent pose at  $f$ .

#### 3.3.3 Normal-line based Navigation (NLBN)

NLBN is utilized for the precise analysis of potential overlapping structures within crowds. The intuition behind this approach is that while a random viewpoint may often obscure visibility in a dense crowd, there are several vantage points that can still provide a clear view for identifying individuals. These observation points are expected to be above and maintain a certain degree to the center of the crowd, since a top-down view can distinguish overlapping, and perspectives from certain angles can ensure that the targets are in the field of view (FOV) of the agent. To find such observation points, NLBN transfers the crowd detection task into a surface detection task. By fitting surfaces on the crowd distribution, normal lines of the surfaces can be obtained, and view points which fulfill the constraints mentioned above can be accurately calculated by using normal lines.

After achieving global crowd distribution in ATE, NLBN first clusters the crowd point cloud into subregions using a clustering method. This step helps divide the large crowd point cloud into manageable parts, as navigating to each navigation point can be resource-intensive. Next, surfaces are fitted to these subregions based on the point cloud data to obtain normal lines. This process transforms the challenging task of crowd analysis into a more manageable surface analysis. Finally, optimized navigation points are generated based on the normal lines, ensuring they maintain a certain distance



and angle from the crowd surfaces for accurate crowd detection. A viewpoint-based method is employed to confirm that the selected navigation points do not overlap with any obstacles.

In particular, GMM [35] is used to divide the global crowd distribution into manageable subregions. It ensures each sample point in a distribution can be assigned with a cluster. Thus, it can divide any crowd distribution into patches. A parameter  $\epsilon$  is used to determine the size of each GMM cluster.

After the clusters and centers are generated, surfaces are fitted for each patch. Then, for the  $N$ -th cluster, the normal is obtained and represented by  $\mathbf{d}_N^{\text{cluster}}$ . Candidate view directions  $\{\mathbf{d}_{N1}^{\text{view}}, \dots, \mathbf{d}_{Nm}^{\text{view}}\}_N$  are sampled under angular constraints:

$$\frac{\mathbf{d}_N^{\text{cluster}} \cdot \mathbf{d}_{Nm}^{\text{view}}}{\|\mathbf{d}_N^{\text{cluster}}\| \|\mathbf{d}_{Nm}^{\text{view}}\|} = \zeta, \quad (4)$$

where  $\zeta$  is a hyper parameter. These candidate view directions can bring the agent to a optimized observation point by selecting a position along the vector. However, there are two issues: 1) The position may be located on obstacles; 2) The crowd cluster may be out of the agent's FOV. To solve the issues and identify the final navigation points from the potential ones, a simple yet effective technique is proposed. In the process of ATE, each cluster point identified by the counting model processes at least one viewpoint of the agent. The vector connecting the viewpoints and target points firmly indicates navigable space, since the propagation of light naturally points to unobstructed area. Besides, the vector can ensure that the crowd is in the FOV as well, since the target image is identified during ATE. Based on this prior, the ATE viewpoints are used to generate the final navigation points. The ATE view vector is calculated as:

$$\mathbf{d}_N^{\text{ATE}} = \mathbf{x}_N^{\text{ATE}} - \mathbf{x}_N^{\text{cluster}}, \quad (5)$$

where  $\mathbf{x}_N^{\text{ATE}}$  is the navigation point from which the agent finds the cluster center  $\mathbf{x}_N^{\text{cluster}}$  during ATE. Then, the potential navigation directions that are at the minimum angles to the ATE view vectors are selected as the final navigation directions:

$$\mathbf{d}_N^{\text{view}} = \arg \min_m \frac{\mathbf{d}_N^{\text{ATE}} \cdot \mathbf{d}_{Nm}^{\text{view}}}{\|\mathbf{d}_N^{\text{ATE}}\| \|\mathbf{d}_{Nm}^{\text{view}}\|}, \quad (6)$$

and the final navigation point  $\mathbf{x}_N^{\text{view}}$  is calculated by

$$\mathbf{x}_N^{\text{view}} = \mathbf{x}_N^{\text{cluster}} + \eta \cdot \mathbf{d}_N^{\text{view}}, \quad (7)$$

where  $\eta$  is a hyper parameter representing the distance between the agent and the crowd cluster. NLBN ensures

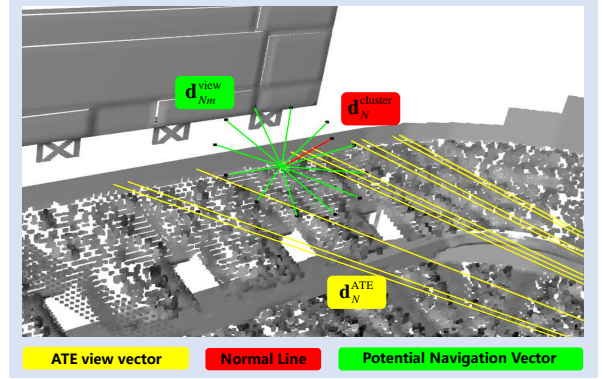


Figure 4: Illustration of the potential navigation vectors, normal lines, and FBE view vectors. Zoom in for better visualization.

close-range, precise target observation and safe navigation, even in complex and unfamiliar environments. The potential navigation vectors, normal lines, and ATE view vectors are illustrated in Figure 4.

### 3.3.4 Fine Detection and Counting (FDC)

Using the navigation points generated by NBLN, the agent travels from one point to another through path planning algorithms. Upon reaching each navigation point, close-range and high-resolution RGB observations can be conducted. These observations are then utilized as inputs for detection models to perform precise target detection. The detection results are projected onto the global point cloud using the depth sensor and the agent pose. To prevent repetitive detections, only one target is retained for each region within a specific scale. Ultimately, the result is calculated by counting the quantity of filtered targets.

## 4. Experiments

### 4.1. Settings

**Metrics.** Mean Absolute Percentage Error (MAPE) is used as the metric to evaluate the counting performance, which is defined as:

$$\text{MAPE} = \frac{1}{M} \sum_{i=1}^M \left| \frac{y_i - \hat{y}_i}{y_i} \right| \times 100\%, \quad (8)$$

where  $M$  is the quantity of testing environments,  $\hat{y}_i$  and  $y_i$  are the estimated count and the ground truth count in an environment, respectively.

The sum of Euclidean distance between adjacent navigation points along the agent traveling path is used to

evaluate the travel distance TD, which is defined as:

$$TD = \sum_{i=1}^{n-1} \|\mathbf{x}_{i+1} - \mathbf{x}_i\|, \quad (9)$$

where  $n$  is the quantity of navigation points in one episode,  $\mathbf{x}_i$  and  $\mathbf{x}_{i+1}$  are the coordinates of the two adjacent navigation points, respectively.

**Implementation Details.** MLLM used in ATE is GPT-4V [46]. The path planning method is A\* algorithm [37]. Altitude is 80m for HAE and 10m for LAE. The crowd density estimator in ATE is Generalized Loss (GL) [41], and the detection model in FDC is Grounding DINO (GD) [34]. For hyper parameters, navigation vector deg  $\zeta$  is 15°, density threshold  $\kappa$  is 0.7, navigation point range  $\eta$  is 8 m, and cluster size  $\epsilon$  is 40.

**Baselines.** We compare ZECC with existing exploration method Frontier-based exploration (FBE) [39], as well as SOTA ZSON methods, 1) CoW [8], 2) OpenFMNav [22]. These methods use advanced foundation models to conduct decision making during navigation. To apply the baselines in ECC, the exploration step limitation for ZSON methods is removed, and they are equipped with GD or GL to conduct crowd counting using the projection method in FDC.

## 4.2. Results

**Overall Performance.** We report overall performance in Table 1. ZECC offers the optimal balance between counting performance and cost. In contrast, FBE delivers the best TD but lacks the ability to perform a target detection function, which limits its capacity for fine observation. This incomplete observation negatively impacts its overall performance. ZSON methods, such as Cow and OpenFMNav come with perception modules; however, they do not select a 3D fine observation point as NLBN, which means they cannot fully observe each individual in the crowd. This limitation leads to individuals being obscured by overlapping crowds, especially when the density is high. In some instances, these methods only identify single individuals, which reduces their efficiency. In contrast, ZECC improves counting efficiency by planning Z-axis exploration using ATE and employing NLBN for detailed detection.

For agents utilizing counting models for crowd counting, the performance tends to be slightly lower than that of agents using detection models. This is due to the increased sparsity of crowd observations as the agents get closer to the crowd. Crowd counting models are mainly trained on images depicting dense crowds, which results in limited generalization capability for scenarios with sparser crowds. Additionally, current ZSON methods do

Method	MAPE (%)	TD (m)
FBE [39] + GL [41]	55.92	2227.71
FBE [39] + GD [34]	53.85	2227.71
CoW [8] + GL [41]	51.19	3271.07
CoW [8] + GD [34]	46.70	3271.07
OpenFMNav [22] + GL [41]	59.71	4936.79
OpenFMNav [22] + GD [34]	46.84	4936.79
ZECC	18.91	3804.63

Table 1: Overall performance of the methods. ZECC achieves best trade-off between MAPE and TD.

	MAPE (%)	TD (m)
ZECC w/o ATE	17.46	4633.67
ZECC w/o HAE	17.46	4633.67
ZECC w/o LAE	88.08	1738.84
ZECC	18.91	3804.63

Table 2: The results of ablation study for components in ATE. w/o ATE refers to using FBE + NLBN results for crowd counting. w/o HAE refers to fix the agent’s altitude to LAE. w/o LAE refers to fix the agent’s altitude to HAE. ZECC improves approximately 17% cost by reducing approximately 8% performance, achieving a better trade-off.

not consider finding a close position for crowd observation, which further degrades performance.

We analyze various environments with different crowd density levels and visualize the average performance and cost of the methods using the GD detector in these scenarios. The results are presented in Figure 5. Among the methods evaluated, ZECC demonstrates the best average performance across different density levels. As crowd density increases, the MLLM in ATE becomes more effective at identifying high-density crowds, resulting in improved performance. In contrast, other methods struggle to manage high-density crowds, leading to limited performance.

In terms of cost, ZECC’s navigation points are influenced by crowd distribution and density. As the density level increases, the cost also rises. Although ZECC falls short of achieving the lowest cost in the last two density levels, its costs are still comparable to the baseline while ensuring effective counting performance. In contrast, other methods do not actively adjust navigation points based on crowd distribution, which results in their costs remaining relatively stable and limits their effectiveness in low-density scenes.

## 4.3. Ablation Study

**ATE.** We conducted ablation studies by removing specific components from the ATE. The results are presented

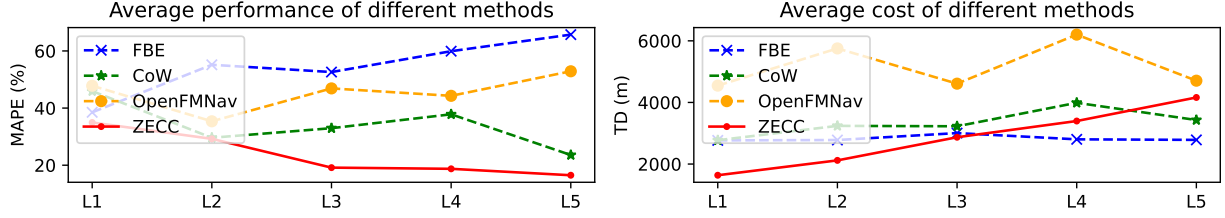


Figure 5: Performance and cost of ZECC and the baselines under different crowd density levels. L1-L5 refers to increasing density level. The figure demonstrate that ZECC achieves a balance between performance and exploration cost.

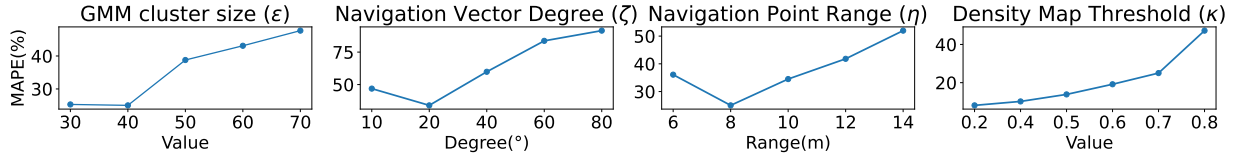


Figure 6: The effect of four hyperparameters used in our model, including GMM cluster size, navigation vector degree, navigation point range and density map threshold.

	MAPE (%)	Successful rate (%)
ZECC w/o NLBN	65.19	100.00
ZECC w/o NL	98.44	8.33
ZECC w/o VPS	92.55	100.00
ZECC w/o ATE-VPS	99.49	1.45
ZECC	18.91	100.00

Table 3: The results of ablation study for components in NLBN. w/o NLBN refers to using ATE results for crowd counting. w/o NL refers to not using normal line (NL) to calculate navigation points but use the cluster centers as navigation points. w/o VPS refers to not using view point selection (VPS) but select a point along the normal vector with  $\eta$ . w/o ATE-VPS refers to not using the ATE-view-vector-based view point selection (ATE-VPS), but randomly select a navigation vector from the potential navigation vectors. Successful rate indicates the ratio of the reachable navigation point reported by the A\* path planning algorithm.

in Table 2. The configuration without ATE (w/o ATE) achieves the best performance because it explores the environments greedily and utilizes NLBN for precise detection, resulting in adequate perception. However, this approach leads to a larger temporal delay (TD). In contrast, ZECC achieves a better balance by conducting both HAE and LAE simultaneously. w/o HAE uses the same setting as w/o ATE. w/o LAE fails for it maintains at a high altitude and does not conduct close range detection, making it hard to capture targets.

**NLBN.** We then conducted ablation studies on NLBN and the results are presented in Table 3. The findings indicate that omitting any component of NLBN results

in a significant drop in either performance or success rates. Without NLBN, the absence of optimized view-points causes ZECC to revert to a ZSON method. When both NL and FBE-VPS are removed, most navigation points end up being located on obstacles, leading to a scarcity of reachable navigation points and incomplete exploration. Additionally, without VPS, the navigation points are positioned directly above the targets, causing the targets to fall out of the field of view, which results in corrupted observations.

#### 4.4. Hyper parameter Study

We then examine the effects of parameters in the method, including GMM cluster size, navigation vector degree, navigation point range, and density map threshold. A gym-like scene featuring a densely packed crowd is utilized to test these parameters. The results are illustrated in Figure 6.

**GMM cluster size.** As the size of the GMM cluster increases, performance tends to deteriorate. When the GMM cluster size is set too low, the method generates sparse navigation points, which prevents the agent from effectively exploring crowded areas, resulting in poor counting performance. Although a smaller GMM cluster size can initially yield high performance, the results become worse when the cluster sizes reach 30 and 40, respectively. Specifically, the cost for a cluster size of 30 is 4065.02 meters, while for a size of 40, it rises to 5125.44 meters. Opting for an extreme GMM cluster size may significantly increase costs without providing substantial improvements in performance. Therefore, it



is crucial to carefully determine the GMM cluster size to find a balance between cost and performance.

**Navigation vector degree.** Performance is optimal at  $20^\circ$ , while it declines at other angles. This degradation occurs because the agent has a limited field of view; it cannot effectively observe targets outside this range. This highlights the importance of our navigation point generation method.

**Navigation point range.** The performance is optimal at a distance of 8 meters, while performance declines at both shorter and longer ranges. A similar trend is observed with the navigation vector degree. At extremely close range, the agent's field of view is restricted, and at long range, the agent is unable to gather detailed observations, which negatively impacts the subsequent target detection phase. Therefore, selecting the right viewpoint and generating appropriate navigation points are crucial for effective scene exploration algorithms.

**Density map threshold.** The results indicate that similar to GMM cluster size, performance declines as the threshold increases. A lower density map threshold results in a coarser estimation of the target zone, which in turn generates more navigation points. This allows for more detailed exploration and observation, leading to improved counting performance. Yet cost rises. For instance, when the density map threshold is 0.7, the travel distance is 4720.02 meters, and it increases to 7272.02 meters when the threshold is 0.4. This is a significant degradation in cost, yet improvement in performance is minor. This emphasizes the importance of parameter selection.

overlap of the crowd. Simultaneously, the estimated navigation points enable obstacle avoidance and ensure that the crowd is in FOV. Experiment results show that ZECC achieves a balance between performance and cost compared to recent navigation agents. Future research will focus on more efficient and scalable agents to enhance performance and adaptability.

## 5. Conclusion

In this study, Embodied Crowd Counting (ECC) is proposed, a task which enables interactive crowd counting. A simulator, the Embodied Crowd Counting Dataset (ECCD) is developed to enable related research for ECC. This dataset includes 60 diverse virtual environments with crowd density modeled by a prior probability distribution, approximating the reality. A method, Zero-shot Embodied Counting (ZECC), is proposed to verify this task. This is an active agent which can explore unknown environments without additional assistance. Active Top-down Exploration (ATE) is proposed to utilize Z-axis moving ability for exploration planning. This module is equipped with MLLM to active high altitude exploration (HAE) or low altitude exploration (LAE), balancing crowd counting performance and exploration cost. Normal-line based Navigation (NLBN) is proposed to select optimized navigation point for crowd observation. This module generates a navigation point from the top-down view and maintains an angle, alleviating

## References

- [1] Garrick Brazil, Abhinav Kumar, Julian Straub, Nikhila Ravi, Justin Johnson, and Georgia Gkioxari. Omni3d: A large benchmark and model for 3d object detection in the wild. *2023 IEEE/CVF Conference on Computer Vision and Pattern Recognition (CVPR)*, pages 13154–13164, 2022.
- [2] Yuri Burda, Harrison Edwards, Amos J. Storkey, and Oleg Klimov. Exploration by random network distillation. *ArXiv*, abs/1810.12894, 2018.
- [3] Angel X. Chang, Angela Dai, Thomas A. Funkhouser, Maciej Halber, Matthias Nießner, Manolis Savva, Shuran Song, Andy Zeng, and Yinda Zhang. Matterport3d: Learning from rgb-d data in indoor environments. *2017 International Conference on 3D Vision (3DV)*, pages 667–676, 2017.
- [4] Guojun Chen, Xiaojing Yu, and Lin Zhong. Type-fly: Flying drones with large language model. *ArXiv*, abs/2312.14950, 2023.
- [5] I-Hsiang Chen, Wei-Ting Chen, Yu-Wei Liu, Ming-Hsuan Yang, and Sy-Yen Kuo. Improving point-based crowd counting and localization based on auxiliary point guidance. In *European Conference on Computer Vision*, 2024.
- [6] Tao Chen, Saurabh Gupta, and Abhinav Kumar Gupta. Learning exploration policies for navigation. *ArXiv*, abs/1903.01959, 2019.
- [7] Daniel Choi, Angus Fung, Haitong Wang, and Aaron Hao Tan. Find everything: A general vision language model approach to multi-object search. *ArXiv*, abs/2410.00388, 2024.
- [8] Samir Yitzhak Gadre, Mitchell Wortsman, Gabriel Ilharco, Ludwig Schmidt, and Shuran Song. Clip on wheels: Zero-shot object navigation as object localization and exploration. *ArXiv*, abs/2203.10421, 2022.
- [9] Samir Yitzhak Gadre, Mitchell Wortsman, Gabriel Ilharco, Ludwig Schmidt, and Shuran Song. Cows on pasture: Baselines and benchmarks for language-driven zero-shot object navigation. *2023 IEEE/CVF Conference on Computer Vision and Pattern Recognition (CVPR)*, pages 23171–23181, 2022.
- [10] Peng Gao, Shijie Geng, Renrui Zhang, Teli Ma, Rongyao Fang, Yongfeng Zhang, Hongsheng Li, and Yu Jiao Qiao. Clip-adapter: Better vision-language models with feature adapters. *ArXiv*, abs/2110.04544, 2021.
- [11] Weina Ge and Robert T. Collins. Marked point processes for crowd counting. In *2009 IEEE Conference on Computer Vision and Pattern Recognition*, pages 2913–2920, 2009.
- [12] Andreas Geiger, Philip Lenz, and Raquel Urtasun. Are we ready for autonomous driving? the kitti vision benchmark suite. *2012 IEEE Conference on Computer Vision and Pattern Recognition*, pages 3354–3361, 2012.
- [13] Saurabh Gupta, Varun Tolani, James Davidson, Sergey Levine, Rahul Sukthankar, and Jitendra Malik. Cognitive mapping and planning for visual navigation. *International Journal of Computer Vision*, 128:1311 – 1330, 2017.
- [14] Bai Lei Gao Junyu Qi Wang Han, Tao and Ouyang Wanli. Dr.vic: Decomposition and reasoning for video individual counting. 2022.
- [15] Chengxi Han, Chen Wu, Haonan Guo, Meiqi Hu, Jiepan Li, and Hongruixuan Chen. Change guiding network: Incorporating change prior to guide change detection in remote sensing imagery. *IEEE Journal of Selected Topics in Applied Earth Observations and Remote Sensing*, pages 1–17, 2023.
- [16] Peter Henry, Michael Krainin, Evan V. Herbst, Xiaofeng Ren, and Dieter Fox. Rgb-d mapping: Using depth cameras for dense 3d modeling of indoor environments. In *International Symposium on Experimental Robotics*, 2010.
- [17] Hanzhe Hu, Zhizhuo Zhou, Varun Jampani, and Shubham Tulsiani. Mvd-fusion: Single-view 3d via depth-consistent multi-view generation. In *CVPR*, 2024.
- [18] Haroon Idrees, Imran Saleemi, Cody Seibert, and Mubarak Shah. Multi-source multi-scale counting in extremely dense crowd images. *2013 IEEE Conference on Computer Vision and Pattern Recognition*, pages 2547–2554, 2013.
- [19] Haroon Idrees, Muhammad Tayyab, Kishan Athrey, Dong Zhang, Somaya Ali Al-Maadeed, Nasir M. Rajpoot, and Mubarak Shah. Composition loss for counting, density map estimation and localization in dense crowds. *ArXiv*, abs/1808.01050, 2018.
- [20] Di Kang and Antoni B. Chan. Crowd counting by adaptively fusing predictions from an image pyramid. *ArXiv*, abs/1805.06115, 2018.
- [21] Di Kang, Zheng Ma, and Antoni B. Chan. Beyond counting: Comparisons of density maps for crowd analysis tasks—counting, detection, and tracking. *IEEE Transactions on Circuits and Systems for Video Technology*, 29:1408–1422, 2017.
- [22] Yuxuan Kuang, Hai Lin, and Meng Jiang. Openfmnav: Towards open-set zero-shot object navigation via vision-language foundation models. *ArXiv*, abs/2402.10670, 2024.
- [23] Jungdae Lee, Taiki Miyaniishi, Shuhei Kurita, Koya Sakamoto, Daichi Azuma, Yutaka Matsuo, and Nakamasa Inoue. Citynav: Language-goal aerial navigation dataset with geographic information, 2024.
- [24] Chengxin Liu, Hao Lu, Zhiguo Cao, and Tongliang Liu. Point-query quadtree for crowd counting, localization, and more. *2023 IEEE/CVF International Conference on Computer Vision (ICCV)*, pages 1676–1685, 2023.
- [25] Shubo Liu, Hongsheng Zhang, Yuankai Qi, Peng Wang, Yanning Zhang, and Qi Wu. Aerialvln: Vision-and-language navigation for uavs. In *International Conference on Computer Vision (ICCV)*, 2023.
- [26] Yuting Liu, Miaojing Shi, Qijun Zhao, and Xiaofang Wang. Point in, box out: Beyond counting persons in crowds. *2019 IEEE/CVF Conference on Computer Vision and Pattern Recognition (CVPR)*, pages 6462–6471, 2019.
- [27] Yuxing Long, Wenzhe Cai, Hongchen Wang, Guanqi Zhan, and Hao Dong. Instructnav: Zero-shot system for generic instruction navigation in unexplored environment.

- ArXiv*, abs/2406.04882, 2024.
- [28] Arjun Majumdar, Gunjan Aggarwal, Bhavika Devnani, Judy Hoffman, and Dhruv Batra. Zson: Zero-shot object-goal navigation using multimodal goal embeddings. *ArXiv*, abs/2206.12403, 2022.
  - [29] Haoliang Meng, Xiaopeng Hong, Chenhao Wang, Miao Shang, and Wangmeng Zuo. Multi-modal crowd counting via a broker modality. *ArXiv*, abs/2407.07518, 2024.
  - [30] Richard A. Newcombe, Shahram Izadi, Otmar Hilliges, David Molyneaux, David Kim, Andrew J. Davison, Pushmeet Kohli, Jamie Shotton, Steve Hodges, and Andrew William Fitzgibbon. Kinectfusion: Real-time dense surface mapping and tracking. *2011 10th IEEE International Symposium on Mixed and Augmented Reality*, pages 127–136, 2011.
  - [31] Simone Parisi, Victoria Dean, Deepak Pathak, and Abhinav Kumar Gupta. Interesting object, curious agent: Learning task-agnostic exploration. *ArXiv*, abs/2111.13119, 2021.
  - [32] Rui Qiu, Ming Xu, Yuyao Yan, Jeremy S. Smith, and Xi Yang. 3d random occlusion and multi-layer projection for deep multi-camera pedestrian localization. *European Conference on Computer Vision 2022*, 2022.
  - [33] Santhosh K. Ramakrishnan, Aaron Gokaslan, Erik Wijmans, Oleksandr Maksymets, Alexander Clegg, John Turner, Eric Undersander, Wojciech Galuba, Andrew Westbury, Angel X. Chang, Manolis Savva, Yili Zhao, and Dhruv Batra. Habitat-matterport 3d dataset (hm3d): 1000 large-scale 3d environments for embodied ai. *ArXiv*, abs/2109.08238, 2021.
  - [34] Tianhe Ren, Qing Jiang, Shilong Liu, Zhaoyang Zeng, Wenlong Liu, Han Gao, Hongjie Huang, Zhengyu Ma, Xiaoke Jiang, Yihao Chen, Yuda Xiong, Hao Zhang, Feng Li, Peijun Tang, Kent Yu, and Lei Zhang. Grounding dino 1.5: Advance the “edge” of open-set object detection. *ArXiv*, abs/2405.10300, 2024.
  - [35] Luca Scrucca, Mohammed Saqr, Sonsoles L’opez-Pernas, and Keefe Murphy. An introduction and tutorial to model-based clustering in education via gaussian mixture modelling. 2023.
  - [36] Vishwanath A. Sindagi, Rajeev Yasarla, and Vishal M. Patel. Jhu-crowd++: Large-scale crowd counting dataset and a benchmark method. *IEEE Transactions on Pattern Analysis and Machine Intelligence*, 44:2594–2609, 2020.
  - [37] Jakub Smolka, Kamil Miszta, Maria Skublewska-Paszkowska, and Edyta Łukasik. A\* pathfinding algorithm modification for a 3d engine. *MATEC Web of Conferences*, 2019.
  - [38] Shuran Song, Samuel P. Lichtenberg, and Jianxiong Xiao. Sun rgb-d: A rgb-d scene understanding benchmark suite. *2015 IEEE Conference on Computer Vision and Pattern Recognition (CVPR)*, pages 567–576, 2015.
  - [39] Anirudh Topiwala, Pranav Inani, and Abhishek Kathpal. Frontier based exploration for autonomous robot. *ArXiv*, abs/1806.03581, 2018.
  - [40] Johanna Wald, Armen Avetisyan, Nassir Navab, Federico Tombari, and Matthias Nießner. Rio: 3d object instance re-localization in changing indoor environments. *2019 IEEE/CVF International Conference on Computer Vision (ICCV)*, pages 7657–7666, 2019.
  - [41] Jia Wan, Ziquan Liu, and Antoni B Chan. A generalized loss function for crowd counting and localization. In *Proceedings of the IEEE/CVF conference on computer vision and pattern recognition*, pages 1974–1983, 2021.
  - [42] Chenhao Wang, Xiaopeng Hong, Zhiheng Ma, Yupeng Wei, Yabin Wang, and Xiaopeng Fan. Multi-modal crowd counting via modal emulation. *ArXiv*, abs/2407.19491, 2024.
  - [43] Qi Wang, Junyu Gao, Wei Lin, and Xuelong Li. Nwpu-crowd: A large-scale benchmark for crowd counting and localization. *IEEE Transactions on Pattern Analysis and Machine Intelligence*, 43:2141–2149, 2020.
  - [44] Tai Wang, Xiaohan Mao, Chenming Zhu, Runsen Xu, Ruiyuan Lyu, Peisen Li, Xiao Chen, Wenwei Zhang, Kai Chen, Tianfan Xue, Xihui Liu, Cewu Lu, Dahua Lin, and Jiangmiao Pang. Embodiedscan: A holistic multi-modal 3d perception suite towards embodied ai. *2024 IEEE/CVF Conference on Computer Vision and Pattern Recognition (CVPR)*, pages 19757–19767, 2023.
  - [45] Xiangyu Wang, Donglin Yang, Ziqin Wang, Hohin Kwan, Jinyu Chen, Wenjun Wu, Hongsheng Li, Yue Liao, and Si Liu. Towards realistic uav vision-language navigation: Platform, benchmark, and methodology. *ArXiv*, abs/2410.07087, 2024.
  - [46] Zhengyuan Yang, Linjie Li, Kevin Lin, Jianfeng Wang, Chung-Ching Lin, Zicheng Liu, and Lijuan Wang. The dawn of lmms: Preliminary explorations with gpt-4v(ision). *ArXiv*, abs/2309.17421, 2023.
  - [47] Yuan Yao, Ao Zhang, Zhengyan Zhang, Zhiyuan Liu, Tat seng Chua, and Maosong Sun. Cpt: Colorful prompt tuning for pre-trained vision-language models. *ArXiv*, abs/2109.11797, 2021.
  - [48] Jiazhao Zhang, Kunyu Wang, Rongtao Xu, Gengze Zhou, Yicong Hong, Xiaomeng Fang, Qi Wu, Zhizheng Zhang, and Wang He. Navid: Video-based vlm plans the next step for vision-and-language navigation. *ArXiv*, abs/2402.15852, 2024.
  - [49] Qi Zhang and Antoni B. Chan. Wide-area crowd counting: Multi-view fusion networks for counting in large scenes. *International Journal of Computer Vision*, 130:1938 – 1960, 2020.
  - [50] Qi Zhang, Yunfei Gong, Daijie Chen, Antoni B. Chan, and Hui dan Huang. Multi-view people detection in large scenes via supervised view-wise contribution weighting. *ArXiv*, abs/2405.19943, 2024.
  - [51] Yingying Zhang, Desen Zhou, Siqin Chen, Shenghua Gao, and Yi Ma. Single-image crowd counting via multi-column convolutional neural network. *2016 IEEE Conference on Computer Vision and Pattern Recognition (CVPR)*, pages 589–597, 2016.
  - [52] Haoran Zhao, Fengxing Pan, Huqiyue Ping, and Yaoming Zhou. Agent as cerebrum, controller as cerebellum: Implementing an embodied Imm-based agent on drones. *ArXiv*, abs/2311.15033, 2023.

- [53] Gengze Zhou, Yicong Hong, and Qi Wu. Navgpt: Explicit reasoning in vision-and-language navigation with large language models. In *AAAI Conference on Artificial Intelligence*, 2023.